

Reprinted with permission from the publisher:

IEEE Transactions on Magnetics

The original publication is available at: <http://ieeexplore.ieee.org>

Copyright © 2006 Institute of Electrical and Electronics Engineers (IEEE)

This material is posted here with permission of the IEEE. Such permission of the IEEE does not in any way imply IEEE endorsement of any of Helsinki University of Technology's products or services. Internal or personal use of this material is permitted. However, permission to reprint/republish this material for advertising or promotional purposes or for creating new collective works for resale or redistribution must be obtained from the IEEE by writing to pubs-permissions@ieee.org.

By choosing to view this document, you agree to all provisions of the copyright laws protecting it.

Publication 2

Dlala, E., Saitz, J., Arkkio, A., “Inverted and forward Preisach models for numerical analysis of electromagnetic field problems”, *IEEE Transactions on Magnetics*, Vol. 42(8): 1963-1973, August 2006.

Inverted and Forward Preisach Models for Numerical Analysis of Electromagnetic Field Problems

Emad Dlala¹, Julius Saitz², and Antero Arkkio¹

¹Laboratory of Electromechanics, Helsinki University of Technology (HUT), FIN-02015 HUT, Finland

²Ansoft Corporation, El Segundo, CA 90245 USA

This paper discusses the use of the inverted (B -based) Preisach model and its incorporation into the finite-element method (FEM). First, the B -based Preisach model is studied thoroughly along with the forward (H -based) Preisach model, highlighting the advantages and disadvantages of both models. The study confirms that, in addition to the main purpose of the B -based model—to compute the magnetic field H directly—the B -based model can overcome the congruency problem. Thus, the B -based model proves to be more accurate than the H -based model. Second, the paper suggests that incorporating the B -based Preisach model into FEM models results in relatively accurate, computationally efficient simulations. The method has been validated by simulating hysteresis torque in a high-speed induction motor, and a comparative investigation of the effectiveness, accuracy, and efficiency of the models has been conducted.

Index Terms—Congruency, finite-element method (FEM), forward (H -based) Preisach model, inverted (B -based) Preisach model, magnetic hysteresis.

I. INTRODUCTION

INCORPORATING hysteresis models into electromagnetic field equations would mostly result from the accuracy of these models to predict the magnetic material behavior correctly. However, only accurate but inefficient models of hysteresis are usually undesirable. In the past few years, significant research effort has been put into the simulation and optimization of high-efficiency hysteresis-incorporative finite-element-method (FEM) codes [1]–[3]. Even though one may find several papers dealing with the incorporation of a hysteresis model into a FEM code, these techniques have not generally been taken up by commercial electromagnetic software producers. Usually, the material capabilities of the commercial softwares are limited only to the single-valued data of the magnetization characteristics.

In FEM formulations, employing the magnetic vector potential A as the unknown, the magnetic flux density B is directly obtained as output quantity [4]–[7]. Most of the well-known hysteresis models, such as the Preisach model and the Jiles–Atherton model [3], are standardly H -based (forward); thus, they are not suitable for modeling hysteresis when coupled with the B -oriented FEM equations because the models have to be inverted in order to be suited for the problem.

A crucial theme in this regard focuses on how to distinguish between what quantity we have at hand as a given, the input $u(t)$ or the output $y(t)$, and what quantity, the input $u(t)$ or the output $y(t)$, is desired to be acquired out of the overall system. In other words, the argument is whether the hysteresis model is needed to be applied in a *forward* manner or in an *inverse* manner. An inverse hysteresis operator Υ is the operator that when applied on the output from a forward hysteresis operator Γ gives the identity operator \mathbf{I} : the composition of the two operators reproduces the original signal [8]

$$\Upsilon[\Gamma[u(t)]] = \Upsilon\Gamma[u(t)] = \Gamma^{-1}\Gamma[u(t)] = \mathbf{I}[u(t)] = u(t). \quad (1)$$

The notion of “inverse” of a hysteresis model has been addressed by many authors proposing a small but important variety of techniques [9]–[13]. The type of a hysteresis model is fundamentally characterized by its hysteron operator. The most basic and common are the *stop*, *relay*, and *play* operators [14]. They are basic because they constitute the simplest hysteresis operator for some other hysteresis models, such as the Prandtl–Ishlinskii model [9] and the Preisach model [15]. The Preisach model consists of a weighted superposition of the relay operators. Equivalently, the Preisach model can be similarly represented by the play operator [16]. Under specific conditions, the stop-type models can operate to approximate the inverse of a given hysteresis model. However, these conditions cannot be readily satisfied especially for the *generalized stop* operator [9], [11].

Efficient implementation of the B -oriented, hysteresis-incorporative FEM analyses would intuitively involve developing methods to find the inverse of a given hysteresis model. In this context, some pioneering works that have dealt with these methods have emerged from two research groups [10]–[13]. Their methods are based on constructing different hysteresis models from the stop and play operators.

Although inverting the Preisach model in a straightforward fashion, as described by (1), seems to be the ideal approach for B -oriented FEM formulations, the inverse of a Preisach model constructed from the “relay” operator is difficult to identify and, therefore, several alternative approaches have been proposed which can be useful for B -oriented FEM formulations. It is found that iterative methods are typically employed to invert the forward Preisach model in which computing the magnetic field H is based on *locally* inverting the hysteresis models by means of iteration (e.g., the Regula–Falsi method [6], [7], [17]–[20]) during the process of simulation. This mechanism requires substantial amounts of computation for obtaining converged solutions—may reach 90% of the total CPU time [6]—and thus the computation of H from B is inefficiently treated.

Other works found in literature dealing with the B -oriented FEM formulations are assigned to reformulating the electromagnetic problem with the constitutive equations. A first direct

approach [21], [22], proposed by Gwan-Soo Park *et al.* to cope with instability, can be appropriate for certain problems, but is not generally attractive, especially in numerical field problems that involve soft magnetic materials in which the magnetic field H becomes too small compared to the magnetization M [23]. An improved finite-element approach which modifies the constitutive equation is introduced in [24], but it also involves iteration steps. An H -version of the fixed-point technique introduced in [25] and further developed by Bottauscio *et al.* [26], [27] is suitable to formulate the electromagnetic problem, resulting in omitting the inversion of the hysteresis model. Another very recent approach [28], called the implicit inverse hysteresis model and based on the Newton–Raphson technique, may not be straightforward to incorporate into simulation programs and is not efficient enough to implement since it also implicates iteration.

Another method made by Takahashi *et al.* [29] to approximate the inverse of the Preisach model by computing the inverse of the Preisach distribution function is B -based. The method uses the flux density B as the input so that the magnetic field H is directly calculated without iteration.

In this paper, we rigorously study the B -based hysteresis model of Preisach type [29] in terms of accuracy and efficiency. The B -based Preisach model clearly has the potential to reduce the computation burden significantly when used with FEM models. However, developing the B -based model imposes modifications to the Preisach model. Thus, it is important that the problems of accuracy and properties of the B -based Preisach model as well as the identification procedure of its vector model be investigated.

The second objective of this paper deals with incorporating the B -based Preisach model into FEM analysis in order to examine its robustness and efficiency. The B -based model will be incorporated into the FEM techniques previously reported in [5] and [30]. For the sake of comparison, we extend our investigation to incorporate the H -based Preisach model into the FEM analysis likewise. The B -version of the fixed-point technique [4], [25], [31] will be the interface between the hysteresis engine and the FEM solution. It will be shown that by using the B -based hysteresis model, we can allow the FEM code to solve electromagnetic fields accurately and efficiently.

The results of the FEM simulations are verified by analyzing hysteresis torque in a high-speed induction motor so that the developed numerical codes are validated with measurement.

II. IDENTIFICATION PROBLEMS OF THE PREISACH MODEL

The identification method of a hysteresis model plays an important role in enhancing the modeling accuracy. In general, hysteresis modeling is indeed very complicated due to the nonsymmetric multivalued branching of hysteresis curves, and simply, it is difficult to find a method, numerical or analytical, that would accurately and generally identify the Preisach model.

Among several Preisach-type models, the classical Preisach model has been extensively used in FEM applications. The main advantages of the classical Preisach-type model over other Preisach-type models relate to its fastness and robustness when FEM field problems are considered, also its simplicity since it represents the basic form of all other Preisach-types [15]. In magnetic applications, the output $y(t)$ of the classical

Preisach model represents the magnetic flux density B and often expressed by the following formula:

$$B(t) = \Gamma[H(t)] = \int_{\alpha \geq \beta} \int \mu(\alpha, \beta) [\hat{\gamma}_{\alpha\beta} H](t) d\alpha d\beta \quad (2)$$

where $[\hat{\gamma}_{\alpha\beta} H](t)$ is the relay operator, sometimes referred to as an elementary Preisach hysteron since it is a basic block from which the Preisach operator $\Gamma[H]$ is constructed. Here α and β correspond to increasing and decreasing values of the input $H(t)$. The output $B(t)$ is determined by summing up the individual contributions of each relay operator $[\hat{\gamma}_{\alpha\beta} H](t)$ weighted by a Preisach distribution function $\mu(\alpha, \beta)$ and integrated over suitable values of α and β .

Commonly, the classical Preisach model (2) is conveniently implemented by means of the Everett integrals in order to circumvent the time-consuming evaluation of the double integral and avoid the differentiation of the experimental data. The output B of the H -based Preisach model is computed following the numerical procedure described in [15], [32]

$$B = -E(-H_0^+, H_0^-) + 2 \sum_{k=1}^n E(H_k^+, H_{k-1}^-) - E(H_k^+, H_k^-) \quad (3)$$

where $E(H_k^+, H_k^-)$ is the Everett function corresponding to the specific reversal points $k = 1, 2, \dots, n$ of the magnetic field H and $E(-H_0^+, H_0^-)$ is the Everett weight of the demagnetizing state. The superscripts $(+, -)$ refer to the increasing and decreasing values of the input H . The Everett function $E(H^+, H^-)$ is constructed from the first-order reversal curves (Fig. 1) according to

$$E(H^+, H^-) = \frac{1}{2}(B_{(H+H^-)} - B_{H+}). \quad (4)$$

The modeling accuracy of the H -based model (3) is generally sensitive to the position of the *reversal points* of the magnetic field H [33], [34]. These problems are associated with the identification method (see, e.g., [35], [36]), specifically with the technique that employs the first-order reversal curves [34]. The problems are induced by the drawbacks of the interpolative procedure (which provokes the congruency problem) carried out in the discrete Preisach plane (the Everett table). The congruency problem has been thoroughly explored by S. Zirka *et al.* in [36], and it is interesting to recognize in [36] that due to the complexity of the problem most of the techniques [33], [37], [38] have not been consistently successful to overcome the problem.

The H -based model works to interpolate the modeled branches from the Everett function where all curves starting from the reversal points with the same field H have the same shape. In most magnetic materials, due to the *relative* large change of the magnetization (dB/dH) near the coercive field (Fig. 2), most of the reversal points are strongly localized near the coercive field. Therefore, only the larger loops which are close to saturation could be improved by the use of first-order reversal curves, and for the minor loops which shrink inside the major loop, the congruency problem would then appear as a major drawback. (The tracing line in the Preisach plane is located around the coercive field.)

On the other hand, the B -based model interpolates the modeled branches where all curves starting with the same flux B

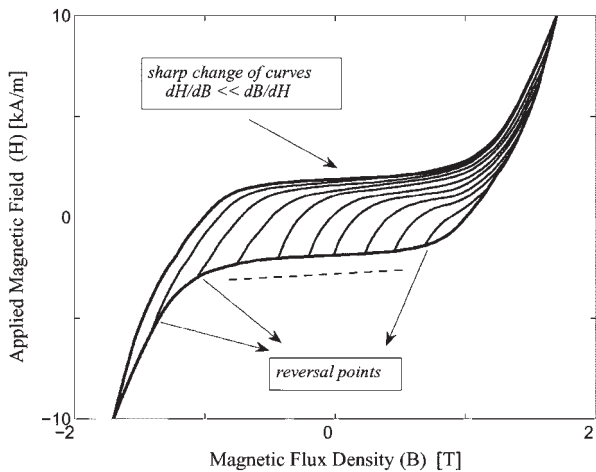


Fig. 1. First-order reversal curves measured on a sample of semihard magnetic material.

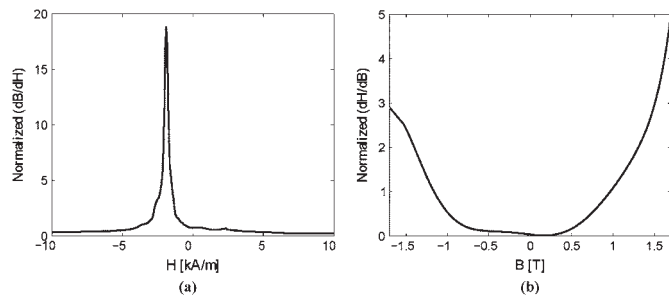


Fig. 2. Relative slopes of magnetization calculated on the ascending branch of the major loop of Fig. 1. (a) Fast abrupt change dB/dH has a maximum near coercivity where most of first-order reversal curves are concentrated. (b) Smooth change dH/dB along the B axis where first-order reversal curves are distributed.

have the same shape. To illustrate that this property clearly enhances the accuracy of the predicted curves, we shall study the B -based model in more detail considering the experimental data of the *semihard* magnetic material. The measurements of hysteresis curves were made using *Labview* program package following a rigorous method provided in [39], [40]. We choose to apply the identification procedures to describe semihard magnetic material as it is required to proceed with the FEM analysis of the high-speed induction motor. However, the concept and ideas of the entire discussions can be immediately applied to describe *soft* and *hard* magnetic materials.

A. The B -Based Model

Using the flux density B as the input variable for the Preisach model implies the possibility to modify the properties of the identification procedure and hence the accuracy of the model. It is imperative to realize that having a *monotone* Everett function is a necessary condition to make the B -based model work sensibly. Satisfying this condition with a hysteresis operator means that the output of such a monotone operator has local extrema that all correspond to the local extrema of its input at exactly the same time instants. This is a highly appreciated consequence of the monotone Everett function: it allows to maintain the *wiping-out* property of the Preisach model. Therefore, the Everett function can be, in principle, computed from the input extrema (first-order reversal curves) of the flux density B . When

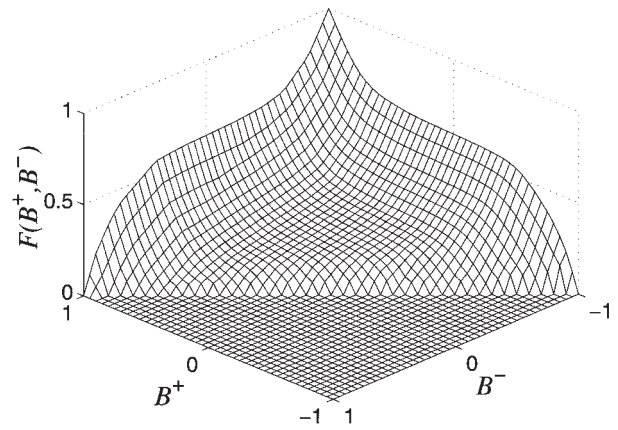


Fig. 3. Normalized inverted Everett function composed from first-order curves of semihard material.

we do so, the formula (4) to construct the Everett function is just *flipped* (inverted) and thus called the inverted Everett function

$$F(B^+, B^-) = \frac{1}{2} (H_{(B+B^-)} - H_{B^+}). \quad (5)$$

Consequently, the B -based Preisach model can be expressed by the following formula:

$$H = -F(-B_0^+, B_0^-) + 2 \sum_{k=1}^n F(B_k^+, B_{k-1}^-) - F(B_k^+, B_k^-) \quad (6)$$

where $F(B_k^+, B_k^-)$ is the inverted Everett function (Fig. 3) corresponding to the specific reversal points $k = 1, 2, \dots, n$ of the scalar magnetic flux density B , and $F(-B_0^+, B_0^-)$ is the inverted Everett weight of the demagnetizing state. The superscripts $(+, -)$ refer to the increasing and decreasing values of the input B , respectively.

Because the inverted Everett function (Fig. 3) used to identify the B -based model (6) is computed from the input extrema of the flux density B , the first-order reversal curves, which are used in the identification, can be reproduced exactly; the same case as in the H -based model.

In the B -based model, the interpolation is controlled by the axis of the flux density B ; the projection on the B axis specifies which pattern should correspond to the modeled curve. Therefore, in contrast to the H -based model, the B -based model is not influenced by the sharp change of the magnetization near the coercive field. The reversal points are lying on the descending (or ascending) branch of the major loop (Fig. 1). Even though the same first-order reversal curves are used to identify the H -based model and the B -based model, the “reversal points” are relatively uniformly distributed with respect to the magnetic flux B while sharply jumping with respect to the magnetic field H . This observation is illustrated in Fig. 2; the relative change dB/dH with respect to H is much sharper than the relative change dH/dB with respect to B .

We should now clarify how and why the accuracy of the B -based model is improved as a consequence of such a note. It is important to predicate our analysis on general regularities which are observed in real magnetization processes. These useful regularities were reported in the early twentieth century known as Madelung’s rules and also restated in [36]. One important qualitative rule of these regularities is the *return-point* memory: if

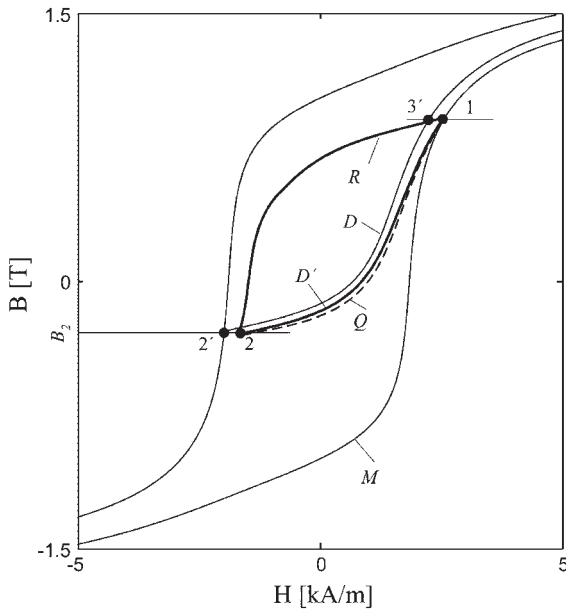


Fig. 4. B -based Preisach model tested against the return-point memory rule. The pattern $2'-3'$ corresponding to the first-order reversal curve D is shifted along the B axis to represent the modeled curve D' , and compared to its equivalent experiment Q (dashed).

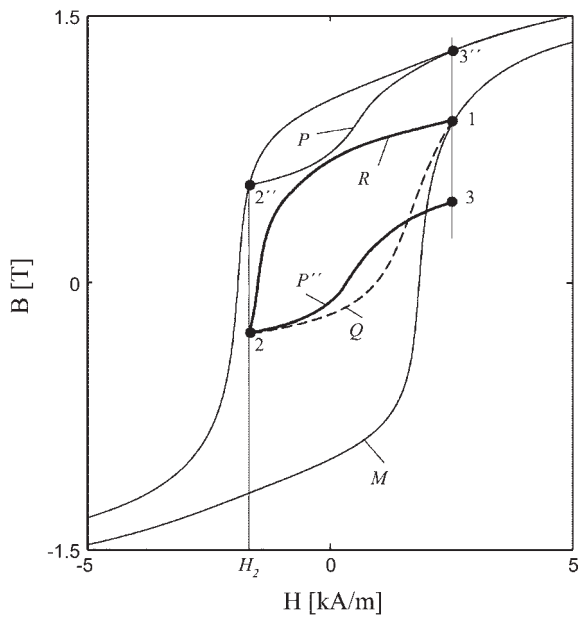


Fig. 5. H -based Preisach model tested against the return-point memory rule. The pattern $2''-3''$ corresponding to the first-order reversal curve P is shifted along the H axis to represent the modeled curve P'' , and compared to its equivalent experiment Q (dashed).

any curve originated from a reversal point, say r_1 , is reversed at another point, say r_2 , then this new curve must return to the initial point r_1 . Dealing with the B -based model, in most cases, this rule can be either satisfied or at least approximated with sufficient accuracy. As we said, in Fig. 4, the first-order reversal curve R originated from point 1 on the major loop M and reversed at point 2 to produce a second-order curve should return to point 1 to satisfy the return-point memory rule. The B -based model reproduces first-order reversal curves exactly and so the first-order reversal curve R . At the reversal point 2, the pattern

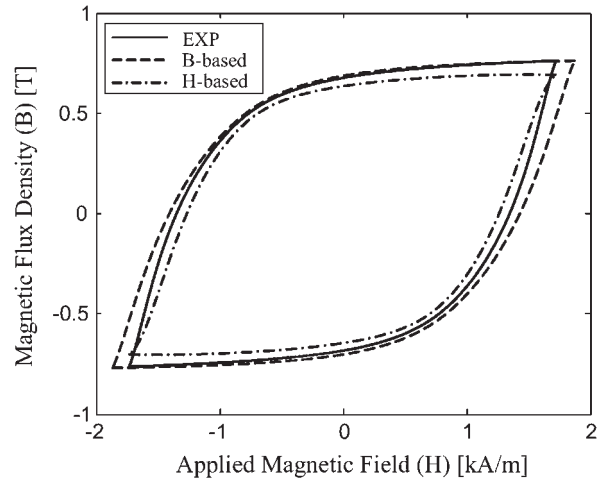


Fig. 6. Symmetrical loops ($H = -1800$ A/m) predicted by the B -based Preisach model, the H -based Preisach model, and compared with experimental data (EXP).

$2'-3'$ of the first-order reversal curve D is copied (shifted) along the B axis, where $B'_2 = B_2$, representing the second-order curve D' . It is clear that the portion D' has fulfilled the return-point memory rule by returning to point 1. This occurred because point 2 is close to point $2'$ (there is no sharp change) and thus, the curve D' should possess an analogous shape to the original (experimental) second-order curve. By carrying out this experiment, it turned out that the curve D' was really a good approximate to the experimental second-order curve Q .

This rule, however, was not satisfied by the H -based model; the curve 1-2 (Fig. 5) was reversed at point 2 and then deviating to reach point 3, which is somewhere in outer space, instead of returning to point 1. When the descending first-order curve R (which is reproduced exactly) is reversed at point 2, a curve P'' is constructed to reach point 3. The resulting second-order curve, P'' , is constructed by interpolating or shifting the first-order curve originating from the same field value of $H_2 = H_2''$ (the model is H -based). Thus, the curve P'' is the pattern of the curve P which is originated from the reversal point $2''$. We can see the major discrepancy of the curve P'' with respect to the experimental Q . Here, the result of the fast change in magnetization is damaging, allowing the congruency problem to take place and undermine the accuracy of the modeled curve P'' .

B. Comparative Results and Discussion

The H -based model (3) and the B -based model (6) were identified from the first-order reversal curves shown in Fig. 1, using the Everett function and the inverted Everett function, respectively. To evaluate the accuracy of the models, two minor loops were measured and compared to their model predictions. Deliberately, these two loops were carefully measured to be located near the coercive field and symmetric (actually we enforced the curves to be symmetric in order to obtain closed minor loops by modeling, which can be meaningfully compared with experimental curves). In the first loop (Fig. 6), the starting field value was very close to the coercive field ($H = -1800$ A/m, $B = -0.75$ T). In the second loop, the starting field value was -1500 A/m slightly higher than the coercive field, and the flux density was -0.45 T as depicted in Fig. 7.

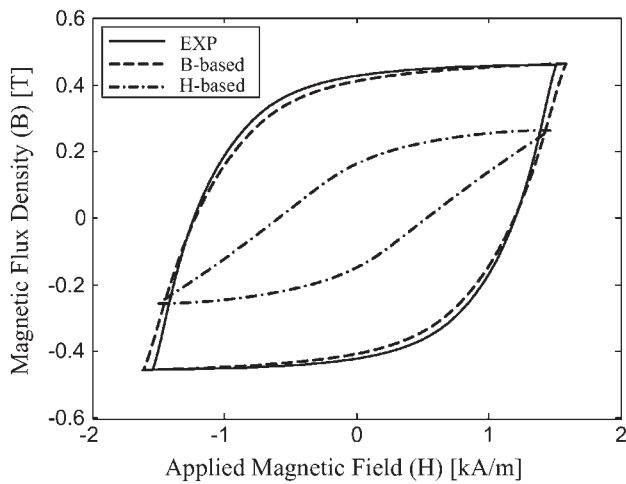


Fig. 7. Symmetrical loops ($H = -1500$ A/m) predicted by the B -based Preisach model, the H -based Preisach model, and compared with experimental data (EXP).

It is readily clear that the B -based model showed more accurate modeling than that of the H -based model for the two loops, especially in the second loop (Fig. 7) in which the effect of congruency is significant. This occurred because the H -based model worked to localize most of the reversal points near the coercive field resulting in unwanted congruent loops. This problem of the H -based is treated in [34] by using the symmetric minor loops instead of the first-order reversal curves to identify the H -based model. This method, however, is able to reproduce only the symmetric loops exactly, and the model is still H -based which is not favored in electromagnetic FEM problems.

In Fig. 8, we carried out a measurement of hysteresis loops caused by applying a cyclic field which started from the demagnetizing state. The measurement is intended to examine the robustness of the H -based model and the B -based model. The results of the two models show excellent agreement with measurement in the region near demagnetization. However, as the field shrank toward smaller loops, the H -based model became more vulnerable to the congruency problem whilst the B -based model kept maintaining relatively agreeable trend.

The idea for describing soft magnetic materials by the B -based model works as successfully as for the semihard magnetic materials. Soft magnetic materials yield incongruent loops the same way as in the semihard magnetic materials. The only difference that for some types of soft magnetic materials the relative change of magnetization near coercivity may be faster and typically the major loop is narrower. Therefore, the B -based model would be suitable for such a case. For other soft magnetic materials (such as soft magnetic composites), because the relative change of magnetization with respect to the magnetic field is not noticeably large, the use of the B -based model would be equally suitable but the H -based model would also perform well. Such studies may require future investigation.

As a result of what has been discussed by far, the B -based Preisach model has demonstrated to be a promising model that can be suitable to cope with the congruency problem. The intrinsic property of the H -based Preisach model is the specific (vertical) H -congruency of the modeled curves. On the other hand, the B -based Preisach model predicts curves that are based on the specific (horizontal) B -congruency. The

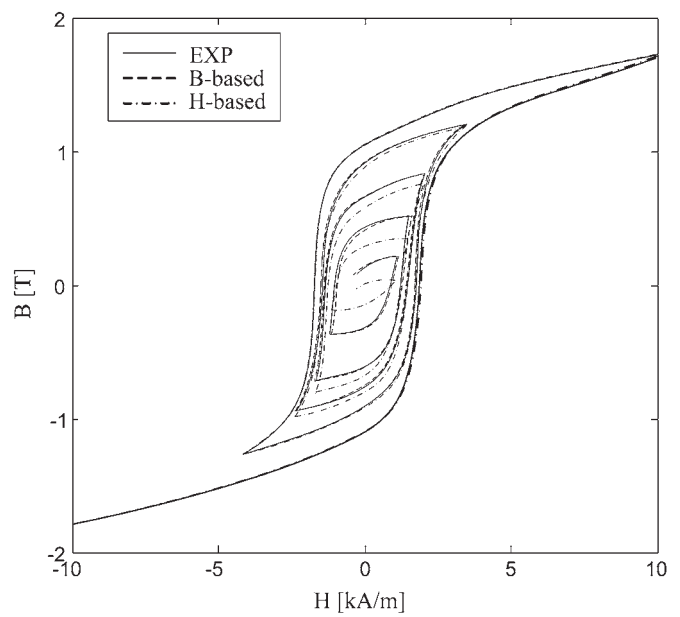


Fig. 8. Hysteretic cyclic loops predicted by the B -based Preisach model, the H -based Preisach model, and compared with experimental data (EXP).

idea to utilize the B -congruency has proven more effective to reproduce curves comparable to experiment. The B -based model is relatively accurate but may have some *minor* discrepancies. Obtaining accurate and general physical modeling of hysteresis requires the development of models that take the H -congruency along with the B -congruency into account: the search of the pattern to be copied (shifted) has to be carried out over the whole B - H plane, not only in the horizontal direction (or in the vertical direction). A non-Preisach model of such competence is proposed by S. Zirka *et al.* [35], [36]. The model is based on transplanting the particular pattern to be modeled from first-order reversal curves, and the model stores previous reversals and hence called history-dependent hysteresis model. The model is exceptionally accurate but may postulate capabilities of interpolation techniques since it searches for the modeled pattern in two directions.

C. The B -Based Vector Model

The scalar model can only describe magnetic fields alternating in one direction. To account for rotating fields, such as the ones revolving in electric rotating machines, the extension of the scalar model to a vector model is needed. The semihard magnetic material to be modeled is nonoriented and, therefore, the *isotropic* vector model can be reasonably used.

The vector model introduced in [15] consists of angularly distributed scalar models, and its identification is based on the scalar model as described in [41]. The magnetic field vector \mathbf{H} can be expressed in two dimensions as

$$\mathbf{H} = \int_{-\pi/2}^{\pi/2} \mathbf{e}_\theta B\{B_\theta\} d\theta \cong \sum_{i=1}^N \mathbf{e}_{\theta_i} B\{B_{\theta_i}\} \quad (7)$$

in which $H_\theta = B\{B_\theta\}$ is the scalar magnetic field in the direction \mathbf{e}_θ , and $B_\theta = |\mathbf{B}| \cos(\vartheta_B - \theta)$ is the projected magnetic flux with the direction of the magnetic flux vector \mathbf{B} , specified by ϑ_B . In numerical computations, it is useful to discretize the interval $\theta \in [-\pi/2, \pi/2]$ as $\theta_i = -\pi/2 + (i-1)\pi/N$,

where $i = 1, \dots, N$ and N is the number of directions, i.e., the magnetic field vector is the vectorial sum of the scalar magnetic fields yielded by the individual scalar hysteresis models (6).

The identification process of the B -based vector model (7) has to satisfy a trivial condition: the output of the vector model magnetized along one direction must be equal to the output of the scalar model. After measuring the inverted Everett function in one direction, the trivial condition can be fulfilled between the inverted scalar Everett function and the unknown vector inverted Everett function:

$$F(B_k^+, B_k^-) \cong \sum_{i=1}^N \cos \theta_i F_v(B_k^+ \cos \theta_i, B_k^- \cos \theta_i). \quad (8)$$

Based on this condition, the vector inverted Everett function $F_v(B_k^+, B_k^-)$ can be constructed by using any mathematical approach that should be able to approximate the function $F_v(B_k^+, B_k^-)$ and must satisfy (8). We used the algorithm proposed in [42] and the vector inverted Everett function was approximated as shown in Fig. 9. Finally, for each direction e_θ , the function $F_v(B_k^+, B_k^-)$ will be implemented in (6) to compute the outputs of the associated directions, which will be summed up vectorially using (7).

It should be noted that after implementing condition (8) and applying the algorithm proposed in [42], there was no significant sharp change in the shape of the vector inverted Everett function with respect to the input B (compare Figs. 3 and 9). This consequence makes the B -based vector model also accurate because it advantageously possesses the good properties of accuracy available in the scalar B -based model.

III. FRAMEWORK AND ASSUMPTIONS ON THE ELECTROMAGNETIC PROBLEM

The high-speed induction motor comprises a solid rotor made of a semihard magnetic material which exhibits relatively large hysteresis loops and hence a significant amount of hysteresis torque. Therefore, for example, correct estimation of the hysteresis torque is important to make the electric drives designers control the motor speed more rigorously. This study, however, is not limited to the hysteresis torque estimation (or to one type of application); rather, it is meant to develop a robust, computationally fast FEM model, which is able to accurately compute magnetic field problems in media with hysteresis, and can be easily applied to any problem of interest.

The induction motor under investigation is considered to be a quasi-static magnetic system. The magnetic field of the motor is assumed to be two-dimensional (2-D), independent of the coordinate parallel to the shaft (z -axis). Only the rotor cross section will be used for the computation of the hysteresis torque. The analysis of the hysteresis torque is based on the computation of the magnetic flux densities in the elements of the mesh (Fig. 10) and then using Maxwell stress tensor. The time-stepping solution of the magnetic field behavior is run over two periods of the supply voltage. In the FEM analysis, a rotating field subjected to the rotor is created by imposing a sinusoidal flux on the outer surface of the air gap. This flux then rotates around the rotor periphery at a constant speed and only the *fundamental* wave of the flux is considered.

Neglecting eddy currents in the rotor is acceptable since the measurements were carried out under no-load conditions at very

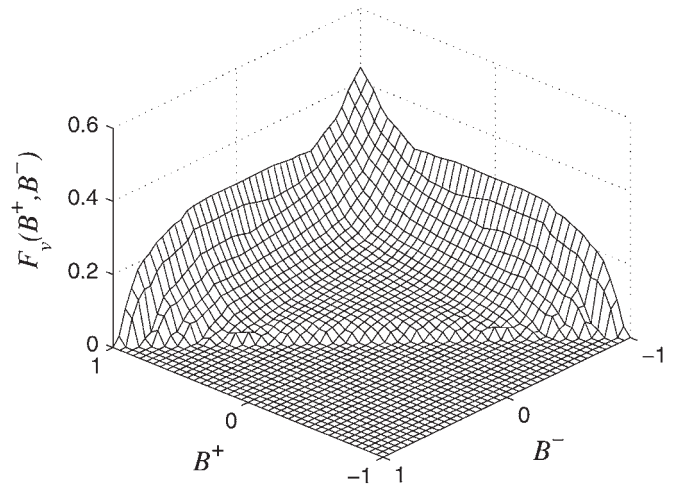


Fig. 9. Normalized vector inverted Everett function with three projections (directions).

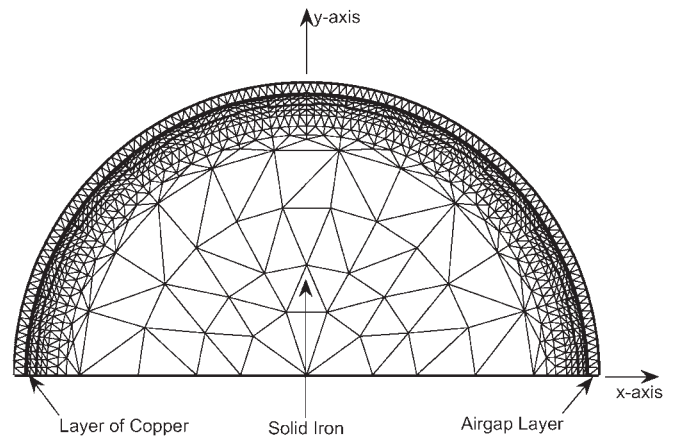


Fig. 10. Finite-element mesh for the considered geometry of the solid rotor.

small slips in the range $\pm(0.02-0.05)\%$ and at low frequency (50 Hz). Therefore, the currents flowing in the copper layer and the iron are disregarded and the copper is modeled as *air*. (The presence of the copper layer had no effect on the computations because all conductivities in the mesh elements were set to zero.) In operational rated conditions (see the Appendix, $f = 500$ Hz), the higher harmonics in the air gap generated by increasing the supply frequency are difficult to penetrate the thick layer of the rotor copper into the iron of the rotor. Therefore, considering only the fundamental component of the air gap flux is reasonable.

The principle of measurement was based on operating the high-speed induction motor at small slips. The only torque or loss component that changes significantly and abruptly when passing the synchronous speed is assumed to correspond to the hysteresis torque. Therefore, by measuring the difference of power that occurs between the motoring and generating modes, the hysteresis torque is determined. The experimental setup is outlined in the Appendix.

IV. FIELD COMPUTATION

In this section, the framework of the electromagnetic field problem presented in the preceding section is transformed into

a computational procedure using FEM analysis. The computational procedure enables to perform the simulation of hysteresis torque acting on the solid rotor of the high-speed induction motor.

A. Magnetic Field Formulation

The interface between the B -based vector model and the FEM solution is established by means of the fixed-point iterative procedure. This nonlinear technique handles the constitutive relationship between the magnetic field intensity \mathbf{H} and the flux density \mathbf{B} , and can be written in the following manner:

$$\mathbf{H} = \nu \mathbf{B} + \mathbf{R} \quad (9)$$

where ν is a properly chosen constant (fixed-point coefficient), and \mathbf{R} is a residual nonlinearity (fixed-point residual), which is to be determined iteratively.

Since only the rotor is considered and all conductivities are equal to zero, the appropriate Maxwell's equations and the constitutive law (9) in terms of the magnetic vector potential \mathbf{A} are formulated as

$$\nabla \times \mathcal{F}(\nabla \times \mathbf{A}) = 0 \quad (10)$$

in which A is the z -component of \mathbf{A} in the x - y plane perpendicular to the shaft. If ν_0 is the reluctivity of the air, the function \mathcal{F} can be defined as

$$\mathcal{F}(B) = \begin{cases} \nu_0 B & \Rightarrow \text{linear regions} \\ \mathcal{H}(B) & \Rightarrow \text{nonlinear hysteretic regions} \\ \nu(|B|) & \Rightarrow \text{nonlinear single-valued regions.} \end{cases} \quad (11)$$

This equation describes the regions from the magnetic material point of view. That is, there are linear elements and nonlinear elements, depending on their replacement in the mesh or more specifically on the nature of the material model describing the B - H behavior in the particular element. The function $\mathcal{H}(B)$ is described by the vector hysteresis model (7) and responsible for the hysteretic part bounded by saturation. Therefore, the relation $\nu(|B|)$ continues from saturation to account for the single-valued region after which hysteresis is no longer subsisting. The relation $\nu(|B|)$ is exponentially approximated and it is also characterized vectorially [5].

After using the weighted-residual method where the test function is chosen to be a shape function N_j taking the boundary conditions into account, the following system of ordinary differential equations of N_a unknown nodal values of the vector potential is obtained from (10):

$$\sum_{i=1}^{N_n} (S_{ij} A_i + P_j) = 0, \quad j = 1, \dots, N_a \quad (12)$$

where

$$S_{ij} = \int_{\Omega} \nu \nabla N_i \cdot \nabla N_j d\Omega;$$

$$P_j = \int_{\Omega} (\mathbf{R} \times \nabla N_j)_z d\Omega.$$

In order to ensure rotating sinusoidal flux on the outer surface of the rotor, the magnetic vector potential must satisfy the following boundary condition:

$$A_b(\phi, t) = \hat{A}_b \sin(p\phi - \omega_r t) \quad (13)$$

where

- A_b z -component of \mathbf{A} on the boundary;
- t time;
- ϕ angle of the particular point on the boundary;
- \hat{A}_b peak value of A_b ;
- p number of pole pairs of the motor;
- ω_r angular slip-frequency.

The amplitude of the vector potential on the boundary is computed from

$$\hat{A}_b = \frac{r}{p} \hat{B} \quad (14)$$

where \hat{B} is the amplitude of the fundamental flux density component in the air gap, and r is the radius of the boundary circle. The value of \hat{B} is determined from the time-harmonic analysis of the motor in which hysteresis is neglected and the iron core is modeled using a single-valued B - H representation.

B. Hysteresis Torque Computation

Since the motor is simulated at no load, we can assume that the electromagnetic torque acting on the periphery of the rotor is only produced by the forces resulting from the hysteresis loss of the rotor material.

The electromagnetic torque is computed through Maxwell stress tensor from a surface integral

$$\mathbf{T}_e = \oint_S \mathbf{r} \times \left\{ \frac{1}{\mu_0} (\mathbf{B} \cdot \mathbf{n}) \mathbf{B} - \frac{1}{2\mu_0} B^2 \mathbf{n} \right\} dS \quad (15)$$

in which μ_0 is the permeability of free space and \mathbf{n} is the unit normal vector of the integration surface S . Using polar coordinates, (15) can be transformed to a line integral along the air gap. As described by Arkkio [30], the line integral can be replaced by a surface integral over the air gap with circle of radius r

$$T_e = \frac{l_{\text{ef}}}{\mu_0(r_{\text{out}} - r_{\text{in}})} \int_{S_{\text{ag}}} r B_r B_\varphi dS \quad (16)$$

where l_{ef} is the effective core length of the motor, and B_r and B_φ stand for the radial and tangential components of the flux density. r_{out} and r_{in} are the outer and inner radii of the air gap, and S_{ag} represents the cross-section area of the air gap.

V. NUMERICAL RESULTS

In this section, the numerical results obtained by implementing the procedures in Sections II and IV will be shown, discussed, and compared with experimental data. A study intended to compare the accuracy and computation time of the B -based vector model and the H -based vector model applied in FEM simulations will be given. The "vector" representation of the H -based model is carried out in the same way described in [42]. All the numerical computations were performed under

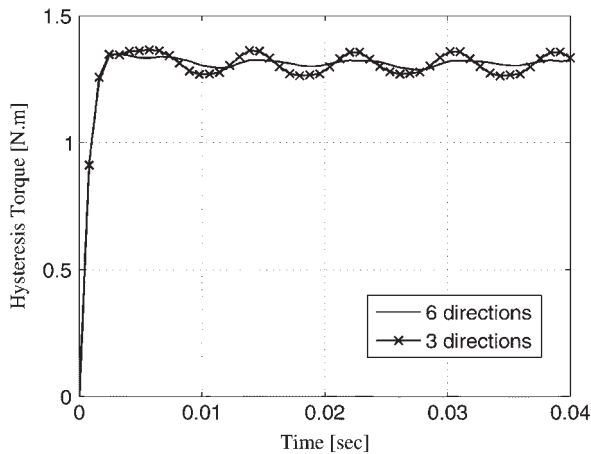


Fig. 11. Instantaneous hysteresis torque computed by the B -based vector model incorporated into FEM model.

Matlab environment, in a Toshiba Satellite R15-S822 1.6-GHz Pentium M 725 Laptop.

The total number of first-order finite elements in the simulated geometry (Fig. 10) was 2023; 906 of which were non-linear and the rest were linear. The peak value of the air gap flux was calculated for each level of the current using time-harmonic method [30].

The magnetic field analysis was initiated by enforcing the rotating sinusoidal flux (13) on the outer surface of the rotor with the amplitude defined by (14), and discretized into 100 time-steps per electrical period. The number of fixed-point iterations was fixed in both cases, the H -based vector model and the B -based vector model. The H -based vector model and the B -based vector model consistently composed of three directions in the computations. Other sets of directions ranged from two to nine directions were investigated and the set of three directions was found to be the most suitable for our simulations in terms of accuracy and computation time points of view. In FEM formulations, the simulation of each element in the mesh requires a hysteretic process for each nonlinear iteration at each time step [5], [32]. The online inversion of the H -based model was optimally realized by a combined bisection-modified Regula-Falsi (BMRF) iterative search [5]. The 2-D numerical interpolation in the vector inverted Everett surface $F_v(B_k^+, B_k^-)$ was facilitated by using 2-D bilinear data interpolation in which B_k^+ and B_k^- were equally spaced, monotonic vectors, specifying the abscissae for the array E_v . The FEM results of the H -based and B -based models have shown convergence for all flux density levels, starting from low values to high values beyond saturation.

A. Accuracy-Related Problems

Since a slotless geometry (solid rotor) was considered, the time variation of the torque was expected to be smooth. As an example, using two electrical periods starting from the zero field as an initial state, the computed instantaneous electromagnetic torque for the amplitude of the fundamental flux component corresponding to 100 A is shown in Fig. 11 using the B -based vector model. It is seen that having six directions in the vector model gave a relatively smooth variation of the torque while having only three directions caused some sinusoidal alternation.

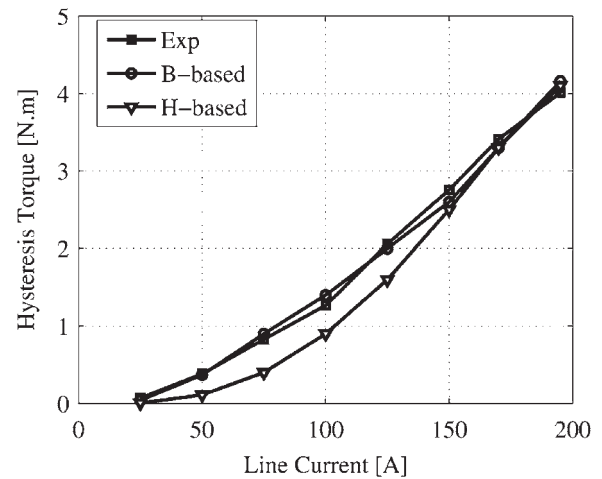


Fig. 12. Estimated hysteresis torque by the H -based vector model and the B -based vector model incorporated into FEM formulation, and compared to the experimental values.

Anyhow, we are mainly concerned about the average value for the steady state of the instantaneous torque—and this is the most common case; those who would need to have smoother trend, it is necessary to use a higher number of directions in the vector model—remembering that this will augment the computational burden and, therefore, will enlarge the computation time.

Similar computations were carried out for currents ranging from 25 up to 195 A. The hysteresis torque was computed and compared with the measured results as presented in Fig. 12; the computed values of the hysteresis torque correspond to the average values of the instantaneous hysteresis torque. This comparison shows that at higher currents the FEM results based on the H -based vector model and on the B -based vector model have given similar good results. At lower currents, however, the FEM H -based model started deviating from the trend of the measured results, while the FEM B -based model was still maintaining almost the same manner of accuracy. The first reason behind the deviation in the H -based model case can be related to the fact that at lower currents the air gap flux was also low—resulting in low values of the corresponding magnetic field computed by the vector model of the H -based model; this occurred because the H -based vector model gave inaccurate predictions at lower values of magnetic fields as it was reported in Section II.

The second reason added to the previous one can be associated with the accumulation of the error calculations resulted from using the BMRF method in inverting the H -based vector model. That is, since the FEM formulation based on the vector magnetic potential gives the flux density at the end of each time step, it is the history of the flux density which is stored when using the B -based vector model. Conversely, when using the H -based model, it is the history of the magnetic field strength that is stored at each time step. This follows that the FEM simulation based on the H -based vector model is notably affected by the accumulative error resulted from inverting the Preisach model by the BMRF method. Keeping in mind that if we attempt to reduce this error to an acceptable level by increasing the number of iterations in the BMRF, it may require a tremendous amount of computation time to achieve a negligibly small percentage of errors.

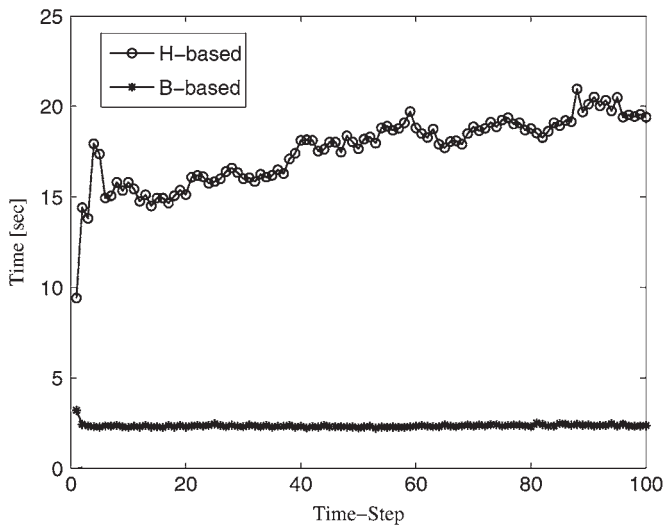


Fig. 13. CPU time consumed on the simulation of the hysteresis torque by the H -based vector model and the B -based vector model incorporated into FEM formulation.

B. Computation-Time-Related Problems

For assessing the computational efficiency, making adequate comparisons between the FEM H -based model and the FEM B -based model requires careful treatment. It is difficult to evaluate the CPU time consumed on the hysteresis models alone without embodying the FEM procedures altogether because the number of the BMRF iterations needed for convergence will depend on the region where the hysteresis element is located in the mesh. Therefore, we intend to globally compare the models for a complete time step including the time consumed on the FEM solution with the fixed-point iteration. In this way, we are able to compare how efficiently the H -based model or the B -based model will perform when incorporating each of them into the FEM models. For the H -based model, the convergence rate of the BMRF method was bounded by setting the relative error to 10%.

In Fig. 13, the CPU time is plotted for one electrical period (100 time-steps) when the level of the air gap flux was 0.21 T, which corresponds to 100 A. It was found that by incorporating the B -based vector model into the FEM models, the overall computational procedure was, in average, 10 times faster compared with that when incorporating the H -based model.

VI. DISCUSSION AND CONCLUSION

In this work, the use of the inverted (B -based) Preisach model and its incorporation into FEM models were of key interest and special importance. We have investigated the accuracy and efficiency of the B -based Preisach model in which scalar and vector hysteresis simulations were examined.

The problems of accuracy in the B -based model were discussed along with the H -based model. The investigation made on the H -based model has led us to discover new ideas about identifying the Preisach model from first-order reversal curves. In addition to the main theme of the B -based model—to compute the magnetic field H directly, it was found that the modeling accuracy of hysteretic curves can be improved by using the inverted Preisach model—thanks to the special mechanism of constructing the inverted Everett function from the first-order curves. Thus, some

TABLE I
MAIN PARAMETERS OF THE HIGH-SPEED INDUCTION MOTOR

Parameter	Value
Number of poles	2
Number of phases	3
Outer diameter of the stator core [mm]	290
Diameter of the solid iron of the rotor [mm]	123
Number of the stator slots	36
Rated voltage [V]	400
Rated power [kW]	200
Rated frequency [Hz]	500
Connection	Delta

promising properties realized in the B -based model can be of great significance to overcome congruency problems.

The fast change of magnetization near the coercivity fields can be problematic because real magnetic materials do not comply with the congruency property. The B -based model is general and able to describe any type of magnetic materials. The B -based model is especially suitable for those materials which greatly deviate from the H -congruency (most magnetic materials).

Computational efficiency was a natural consequence of the straightforward structure of the B -based model since the model gives H directly from B . It was found that by incorporating the B -based vector model into FEM models, the overall computation time was 10 times shorter than that when incorporating the H -based vector model. As a result, the proposed models can be efficiently implemented in the FEM codes intended for the everyday-design purposes of electric machines. However, modifications on the present work remain possible to achieve faster simulation codes. For instance, identifying the B -based model may be performed in a simpler way by using only the major loop instead of a complete family of first-order reversal curves (Fig. 1). A fine grid as used here in the discrete Preisach plane would result in slower 2-D interpolation procedures, increasing the overall computation burden. A reduction of the input data can be obtained by making some assumptions, based on physical groundwork, allowing the B -based model to be identified by means of parametric methods as described by Kadar [43] and in a slightly different way by Naidu [44]. By doing so, we are certain that also, like in the H -based models [43], [44], the computation cost will be alleviated in the B -based model; however, accuracy problems must be investigated beforehand.

A possible shortcoming of the B -based model at present is related to its generalization to describe dynamic hysteresis by using well-developed models such as Bertotti's model [45]. The generalized dynamic model [45] is H -based in which the dipoles are assumed to switch at a finite rate, proportional to the difference between the local magnetic field $H(t)$ and the elementary loop switching fields α and β ; this cannot be straightforward perceived with the B -based model. On the other hand, a viscous-type dynamic hysteresis model [46], [47], which is compatible with any static hysteresis model, can be suitable for the B -based model.

Our future work will envisage more possible extensions of the current models. Such extensions may include eddy currents, dynamic hysteresis, and anisotropic behaviors.

APPENDIX

The tested motor specifications are given in Table I. The hysteresis torque was measured at various values of the line current

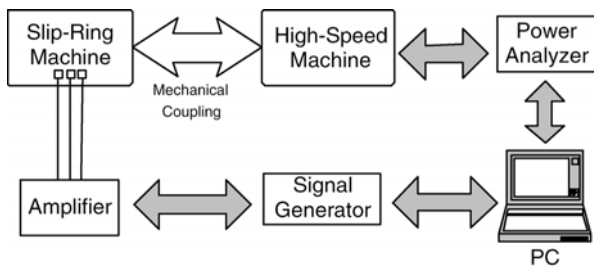


Fig. 14. Experimental setup for measuring hysteresis torque on a high-speed induction motor manufactured at High Speed Tech Oy Ltd.

(25–195 A) while the high-speed induction motor was operated at very small slips, and at a frequency 10 times less than the rated.

The measurement scheme of the hysteresis torque was based on determining the difference of power occurring between motoring and generating modes. The experimental setup used to measure the hysteresis torque is shown in Fig. 14. It consisted mainly of the control circuit and the high-speed induction motor which was mechanically coupled to a slip-ring induction machine. The critical task in this measurement was the accurate frequency control of the current supplied to the slip-ring rotor so the desired small slips were successfully achieved. A control circuit was therefore made for this purpose supervised by a PC as shown in Fig. 14. The entire measurement offset was estimated to be less than 10%.

ACKNOWLEDGMENT

The first author would like to acknowledge the following people for cooperation and useful discussions: Dr. A. Belachen from Laboratory of Electromechanics, Helsinki University of Technology, Finland; Dr. M. Kuczmann from the Institute of Informatics and Electrical Engineering, Széchenyi István University, Hungary; and Prof. A. Iványi from Budapest University of Technology and Economics, Hungary.

REFERENCES

- [1] A. Reimers, M. Gyimesi, E. D. Torre, and D. Ostergaard, "Implementation of the Preisach DOK magnetic hysteresis model in a commercial finite element package," *IEEE Trans. Magn.*, vol. 37, no. 5, pp. 3362–3365, Sep. 2001.
- [2] Y. Bernard, E. Mendes, L. Santandrea, and F. Bouillaul, "Inverse Preisach model in finite elements modeling," *Eur. Phys. J. Appl. Phys.*, vol. 12, pp. 117–121, Aug. 2000.
- [3] N. Sadowski, N. J. Batistela, J. P. A. Bastos, and M. Lajoie-Mazenc, "An inverse Jiles-Atherton model to take into account hysteresis in timestepping finite-element calculations," *IEEE Trans. Magn.*, vol. 38, no. 2, pp. 797–800, Mar. 2002.
- [4] O. Bottauscio, D. Chiarabaglio, M. Chiampi, and M. Repetto, "A hysteretic periodic magnetic field solution using Preisach model and fixed-point technique," *IEEE Trans. Magn.*, vol. 31, no. 6, pp. 3548–3550, Nov. 1995.
- [5] J. Saitz, "Magnetic field analysis of electric machines taking ferromagnetic hysteresis into account," Ph.D. thesis, Acta Polytechnica Scandinavica, 2001.
- [6] J. Saitz, "Computation of the core loss in an induction motor using the vector Preisach hysteresis model incorporated in finite element analysis," *IEEE Trans. Magn.*, vol. 36, no. 4, pp. 769–773, Jul. 2000.
- [7] J. Saitz, "Magnetic field analysis of induction motors combining Preisach hysteresis modeling and finite element techniques," *IEEE Trans. Magn.*, vol. 37, no. 5, pp. 3693–3697, Sep. 2001.
- [8] C. Natale, F. Velardi, and C. Visone, "Identification and compensation of Preisach hysteresis models for magnetostrictive actuators," *J. Phys. B: Condens. Matter*, vol. 306, no. 1–4, pp. 357–363, Dec. 2001.
- [9] M. A. Krasnosel'skii and A. V. Pokrovskii, *Systems with Hysteresis*. New York: Springer-Verlag, 1989.
- [10] G. Miano, C. Serpico, and C. Visone, "A new model of magnetic hysteresis, based on stop hysteresis: An application to the magnetic field diffusion," *IEEE Trans. Magn.*, vol. 32, no. 3, pp. 1132–1135, May 1996.
- [11] S. Bobbio, G. Miano, C. Serpico, and C. Visone, "Models of magnetic hysteresis based on play and stop hysteresis," *IEEE Trans. Magn.*, vol. 33, no. 6, pp. 4417–4426, Nov. 1997.
- [12] T. Matsuo and M. Shimasaki, "Isotropic vector hysteresis represented by superposition of stop hysteresis models," *IEEE Trans. Magn.*, vol. 37, no. 5, pp. 3357–3361, Sep. 2001.
- [13] T. Matsuo, D. Shimode, Y. Terada, and M. Shimasaki, "Application of stop and play models to the representation of magnetic characteristics of silicon steel sheet," *IEEE Trans. Magn.*, vol. 39, no. 3, pp. 1361–1364, May 2003.
- [14] M. Sjöström, "Hysteresis modeling of high temperature superconductors," Ph.D. thesis, Swiss Federal Institute of Technology Lausanne (EPFL), 2001.
- [15] I. D. Mayergoyz, *Mathematical Models of Hysteresis*. New York: Springer-Verlag, 1991.
- [16] M. Brokate, "Some mathematical properties of the Preisach model for hysteresis," *IEEE Trans. Magn.*, vol. 25, no. 4, pp. 2922–2924, Jul. 1989.
- [17] J. J. C. Gyselinck, L. Vandeveld, D. Makaveev, and J. A. A. Melkebeek, "Calculation of no load losses in an induction motor using an inverse Preisach model and an eddy current loss model," *IEEE Trans. Magn.*, vol. 36, no. 4, pp. 856–860, Jul. 2000.
- [18] M. Rosu, J. Saitz, and A. Arkkio, "Hysteresis model for finite-element analysis of permanent-magnet demagnetization in a large synchronous motor under a fault condition," *IEEE Trans. Magn.*, vol. 41, no. 6, pp. 2118–2123, Jun. 2005.
- [19] O. Bottauscio, M. Chiampi, D. Chiarabaglio, and M. Repetto, "A finite element solution for periodic eddy current problems in hysteretic media," *J. Phys. B: Condens. Matter*, vol. 160, pp. 96–97, Jul. 1996.
- [20] F. Henrotte, A. Nicolet, F. Delinck, A. Genon, and W. Legros, "Modeling of ferromagnetic materials in 2d finite element problems using Preisach's model," *IEEE Trans. Magn.*, vol. 28, no. 5, pp. 2614–2616, Sep. 1992.
- [21] G.-S. Park, S.-Y. Hahn, K.-S. Lee, and H.-K. Jung, "Implementation of hysteresis characteristics using the Preisach model with M-B variables," *IEEE Trans. Magn.*, vol. 29, no. 2, pp. 1542–1545, Mar. 1993.
- [22] G.-S. Park, S.-Y. Hahn, K.-S. Lee, and H.-K. Jung, "Practical method to obtain the particle density distribution in scalar Preisach model," *IEEE Trans. Magn.*, vol. 33, no. 2, pp. 1600–1603, Mar. 1997.
- [23] A. Iványi, *Hysteresis Models in Electromagnetic Computation*. Budapest, Hungary: Akadémia Kiadó, 1997.
- [24] H.-K. Kim, S.-K. Hong, and H.-K. Jung, "An improved finite element analysis of magnetic system considering magnetic hysteresis," *IEEE Trans. Magn.*, vol. 36, no. 4, pp. 689–692, Jul. 2000.
- [25] F. Hantila, "A method of solving stationary magnetic field in nonlinear media," *Revue Roumaine des Sciences Techniques, Électrotechnique et Énergétique*, vol. 20, no. 3, pp. 397–407, 1975.
- [26] L. R. Dupr, O. Bottauscio, M. Chiampi, J. Melkebeek, and M. Repetto, "Modeling electromagnetic phenomena in soft magnetic materials under unidirectional time periodic flux excitations," *IEEE Trans. Magn.*, vol. 35, no. 5, pp. 4171–4184, Sep. 1999.
- [27] O. Bottauscio, M. Chiampi, D. Chiarabaglio, and M. Repetto, "Preisach-type hysteresis models in magnetic field computation," *J. Phys. B: Condens. Matter*, vol. 275, no. 1–3, pp. 34–39, Jan. 2000.
- [28] Y. Zhai and L. Vu-Quoc, "Analysis of power magnetic components with nonlinear static hysteresis: Finite-element formulation," *IEEE Trans. Magn.*, vol. 41, no. 7, pp. 2243–2256, Jul. 2005.
- [29] N. Takahashi, S. Miyabara, and K. Fujiwara, "Problems in practical finite element analysis using Preisach hysteresis model," *IEEE Trans. Magn.*, vol. 35, no. 3, pp. 1243–1246, May 1999.
- [30] A. Arkkio, "Analysis of induction motors based on the numerical solution of the magnetic field and circuit equations," Ph.D. thesis, Acta Polytechnica Scandinavica, Sep. 1987.
- [31] M. Chiampi, D. Chiarabaglio, and M. Repetto, "A Jiles-Atherton and fixed-point combined technique for time periodic magnetic field problems with hysteresis," *IEEE Trans. Magn.*, vol. 31, no. 11, pp. 4306–43, Nov. 1995.
- [32] A. Bergqvist, "On magnetic hysteresis modeling," Ph.D. thesis, Royal Institute of Technology, Electric Power Engineering, Stockholm, Sweden, 1994.
- [33] I. D. Mayergoyz, G. Friedman, and C. Salling, "Generalized Preisach model of hysteresis," *IEEE Trans. Magn.*, vol. 24, no. 1, pp. 212–217, Jan. 1988.

- [34] E. Dlala, J. Saitz, and A. Arkkio, "Hysteresis modeling based on symmetric minor loops," *IEEE Trans. Magn.*, vol. 41, no. 8, pp. 2343–2348, Aug. 2005.
- [35] S. E. Zirka and Y. Moroz, "Hysteresis modeling based on similarity," *IEEE Trans. Magn.*, vol. 35, no. 4, pp. 2090–2096, Jul. 1999.
- [36] S. E. Zirka, Y. Moroz, P. Marketos, and A. J. Moses, "Congruency-based hysteresis models for transient simulation," *IEEE Trans. Magn.*, vol. 40, no. 2, pp. 390–399, Mar. 2004.
- [37] V. Basso and G. Bertotti, "Hysteresis models for the description of domain wall motion," *IEEE Trans. Magn.*, vol. 32, no. 5, pp. 4210–4212, Sep. 1996.
- [38] S. F. H. Parker, C. A. Faunce, P. J. Grundy, M. G. Maylin, J. L. C. Ludlow, and R. Lane, "Preisach modeling of magnetization changes in steel," *J. Magn. Magn. Mater.*, vol. 145, pp. 51–56, Mar. 1995.
- [39] P. Kis, M. Kuczmann, J. Fuzi, and A. Ivanyi, "Hysteresis measurement in LabView," *J. Phys B: Condens. Matter*, vol. 343, no. 1–4, pp. 357–363, Jan. 2004.
- [40] E. Dlala and A. Ivanyi, *Measurements of Magnetic Hysteresis Curves in Labview* Budapest, Hungary, May 2005, special assignment.
- [41] O. Bottauscio, M. Chiampi, D. Chiarabaglio, M. Repetto, and C. Ragusa, "Analysis of isotropic materials with vector hysteresis," *IEEE Trans. Magn.*, vol. 34, no. 4, pp. 1258–1260, Jul. 1998.
- [42] M. Kuczmann, "Neural network based vector hysteresis model and the nondestructive testing method," Ph.D. thesis, Budapest University of Technology and Economics, 2004.
- [43] G. Kadar, "On the Preisach function of ferromagnetic hysteresis," *J. Appl. Phys.*, vol. 61, no. 8, pp. 4013–4015, Apr. 1987.
- [44] S. R. Naidu, "Simulation of the hysteresis phenomenon using Preisach's theory," *Inst. Elect. Eng. Proc.*, vol. 137, no. 2, pp. 73–79, Mar. 1990.
- [45] G. Bertotti, "Dynamic generalization of the scalar Preisach model of hysteresis," *IEEE Trans. Magn.*, vol. 28, no. 5, pp. 2599–2601, Sep. 1992.
- [46] S. E. Zirka, Y. I. Moroz, P. Marketos, and A. J. Moses, "Dynamic hysteresis modeling," *Physica B*, vol. 343, no. 1–4, pp. 90–95, 2003.
- [47] S. E. Zirka, Y. I. Moroz, P. Marketos, and A. J. Moses, "A viscous-type dynamic hysteresis model as a tool for loss separation in conducting ferromagnetic laminations," *IEEE Trans. Magn.*, vol. 41, no. 3, pp. 1109–1111, Mar. 2005.

Manuscript received December 1, 2005; revised May 12, 2006. Corresponding author: E. Dlala (e-mail: emad.dlala@hut.fi).

Emad Dlala was born in Libya in 1976. He received the B.Sc. degree in electrical power engineering from Seventh of April University, Sabrata, Libya, in 1999 and the M.Sc. degree (with distinction) in electromechanical energy conversion from Helsinki University of Technology, Finland, in 2005. He is currently pursuing the Ph.D. degree at the Laboratory of Electromechanics, Helsinki University of Technology. His doctoral study involves dynamic hysteresis modeling of steel sheets in electric machines.

Before he joined his M.Sc. study, he had been at an industrial program during 2000–2002 where he was first trained in Malta and then worked in Germany for Fritz Werner Industrie-Ausrustungen GmbH. His research interests include numerical analysis of electromagnetic field problems, measurement and simulation of electric machines, and modeling magnetic material, especially hysteresis and eddy currents.

Julius Saitz was born in Kosice, Slovakia, in 1971. He received the M.S. degree from the University of Zilina, Zilina, Slovakia, in 1995 and the Ph.D. degree from Helsinki University of Technology, Finland, in 2001.

He continued to work at Helsinki University of Technology as a Research Scientist and a Lecturer. In December 2004 he joined Ansoft Corporation, El Segundo, CA, where he currently works as an application engineer. His research interests include numerical analysis of electric machines and other electromechanical systems and modeling of magnetic hysteresis.

Antero Arkkio was born in Vehkalahti, Finland, in 1955. He received the M.Sc. (Tech) and D.Sc. (Tech) degrees from Helsinki University of Technology (TKK), Finland, in 1980 and 1988, respectively.

He has been the Professor of Electrical Engineering (Electromechanics) at TKK since 2001. Before this, he worked as a Senior Research Scientist and Laboratory Manager at TKK. He has worked with various research projects dealing with modeling, design, and measurement of electrical machines.